Ligand Specificity of Human Plasminogen Kringle 4†

Marita R. Rejante, In-Ja L. Byeon, and Miguel Llinás*
Department of Chemistry, Carnegie Mellon University, Pittsburgh, Pennsylvania 15213-3890
Received July 3, 1991; Revised Manuscript Received September 3, 1991

ABSTRACT: The ligand specificity of the human plasminogen kringle 4 was characterized in terms of ligand size, aromatic/aliphatic character, and ionic charge distribution. The binding of the following ligands was investigated via ^{1}H NMR spectroscopy, and their equilibrium association constants (K_a) were determined: (1) *p*-aminomethylbenzoic acid ($K_a \sim 4.8$ mM^{-1}), (2) benzylamine ($K_a \sim 0.2$ mM^{-1}), (3) 1-aminohexane ($K_a \sim 0.07$ mM^{-1}), (4) 7-aminoheptanoic acid ($K_a \sim 6.6$ mM^{-1}), (5) 5-aminopentanoic acid ($K_a \sim 16$ mM^{-1}), (6) N^{α}-acetyl-L-arginine ($K_a \sim 0.3$ mM^{-1}), and (7) N^{α}-acetyl-L-arginine methyl ester ($K_a \sim 0.08$ mM^{-1}). Benzamidine and L-arginine do not bind measurably to kringle 4. We have also established that 1-hexanoic acid and 4-methylbenzoic acid do not interact significantly with kringle 4 ($K_a < 0.05$ mM^{-1}). The Trp^{62} resonances were found to be quite sensitive to aromatic ligands as well as to aliphatic ligand length. Phe^{64} is similarly sensitive to the ligand aromatic/aliphatic character and chain length and to the identity of the ligand anionic group. His^{31} and His^{33} do not respond significantly to variations in ligand structure, although they are perturbed by aromatic and aliphatic effectors. The perturbations induced by the arginine derivatives on these residues show that these compounds interact with the lysine-binding site (LBS) of kringle 4. The LBS was further characterized using 2D NMR studies of a kringle 4/*trans*-(aminomethyl)cyclohexanecarboxylic acid (AMCHA) complex. A complete assignment of the AMCHA spectrum in the bound state was achieved. This enabled the unambiguous identification of intermolecular contact points between the central AMCHA protons and Trp^{62} and Trp^{72}. A model based on the X-ray crystallographic structure of kringle 4, incorporating these constraints, has been derived.

The fibrinolytic proenzyme plasminogen is known to possess a specific affinity for lysine and other ω-aminocarboxylic acids (Brockway & Castellino, 1972; Sottrup-Jensen et al., 1978). In turn, occupancy of the lysine-binding sites (LBSs)[1] of plasminogen causes the conformational changes which facilitate plasminogen activation (Brockway & Castellino, 1972). Furthermore, these sites appear to be involved in the binding of plasminogen to fibrin(ogen) (Thorsen, 1975) and α_2-antiplasmin (Wiman et al., 1978, 1979; Sugiyama et al., 1988; Hortin et al., 1989).

The lysine-binding affinity of plasminogen was found to be localized in its heavy chain (Rickli & Otavsky, 1975; Vâli & Patthy, 1982), a polypeptide composed of five autonomous kringle domains (Castellino et al., 1981). Three of these, kringles 1, 4, and 5, are known to harbor plasminogen's high-, intermediate-, and low-affinity lysine-binding sites, respectively (Lerch & Rickli, 1980; De Marco et al., 1982, 1987; Motta et al., 1987; Petros et al., 1989; Thewes et al., 1990). Although there is a definite correlation between plasminogen's lysine- and fibrin-binding capabilities, the nature of this correlation is not completely clear (Sugiyama et al., 1988). Studies by Suenson and Thorsen (1981) suggest that the intermediate lysine-binding site in plasminogen mediates its initial binding to fibrin. We have also shown that kringle 4 definitely interacts with fibrinogen (Rejante et al., 1991). Thus, characterization and structure elucidation of the LBS in kringle 4 has remained an important facet of the study of plasminogen's interactions with its substrate(s) and inhibitors.

^{1}H NMR spectroscopy has proven to be a most useful tool in the investigation of ligand–kringle interactions because it provides a means of observing residue-specific perturbations accompanying ligand binding (Llinás et al., 1985; De Marco et al., 1986a). It also affords data which can lead to rather accurate estimates of the ligand–kringle equilibrium association constants. These earlier studies focused on the complexation of kringle 4 with aliphatic ligands and *p*-benzylaminesulfonic acid, an aromatic analogue (De Marco et al., 1986a; Ramesh et al., 1987; Petros et al., 1989), and were based mostly on monitoring the shifts of proton resonances in response to ligand additions. Such studies, in combination with computer modeling based on the crystallographic structure of the prothrombin kringle 1, have led to a better understanding of the nature of the kringle 4–ligand interaction (Ramesh et al., 1987; Tulinsky et al., 1988). Recently reported low-resolution ^{1}H NMR (Atkinson & Williams, 1990) and 1.9-Å resolution crystallographic structures of kringle 4 (Mulichak & Tulinsky,

Chart I

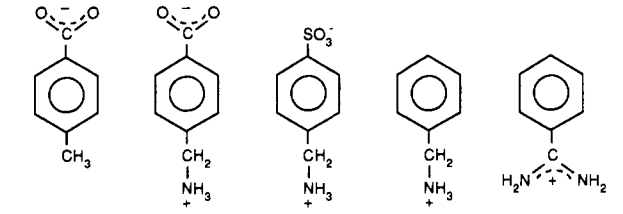

† Research was supported by the US Public Health Service, NIH Grant HL-29409. A grant from the Pittsburgh Supercomputing Center through the NIH Division of Research, Cooperative Agreement 1P41RR06009, is gratefully acknowledged.

[1] Abbreviations: AcArg, N^{α}-acetyl-L-arginine; AMBOC, 4-(aminomethyl)bicyclo[2.2.2]octane-1-carboxylic acid; AMCHA, *trans*-(aminomethyl)cyclohexanecarboxylic acid; BASA, *p*-benzylaminesulfonic acid; CM-Sephadex, carboxymethyl-Sephadex; COSY, two-dimensional chemical shift correlated spectroscopy; FID, free induction decay; LBS, lysine-binding site; NOE, nuclear Overhauser effect; NOESY, 2D NOE spectroscopy; pH*, glass electrode pH reading uncorrected for deuterium isotope effects; PAMBA, *p*-aminomethylbenzoic acid; Photo-CIDNP, photochemically induced dynamic nuclear polarization; t-PA tissue-type plasminogen activator; TPPI, time-proportional phase incrementation; 6-AHA, 6-aminohexanoic acid; 7-AHA, 7-aminoheptanoic acid; 5-APA, 5-aminopentanoic acid; 2D, two dimensional.

0006-2960/91/0430-11081$02.50/0

Chart II

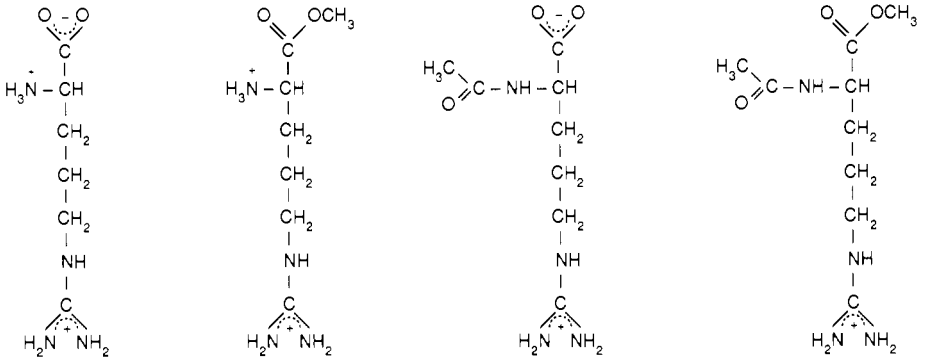

1990) are basically confirmatory of our original model. In this paper, we investigate how various ligands fit at the LBS and correlate their binding behavior with the X-ray crystallographic structure. NOEs observed between kringle 4 and the ligand, *trans*-(aminomethyl)cyclohexanecarboxylic acid (AMCHA), as well as intramolecular kringle 4 NOEs, have been used to derive a detailed picture of the ligand–kringle 4 interaction at atomic level resolution.

The binding studies of various ligands to kringle 4 reported here were designed both to determine the effect of dipole length on binding strength and to discern the kringle 4 resonances responsive to the ligand variability. A number of aliphatic and aromatic ligands, along with chain length variants of 6-AHA, were investigated. These analogues include 5-aminopentanoic acid (5-APA), 7-aminoheptanoic acid (7-AHA), and sets of ligands whose structures represent systematic variations of *p*-benzylaminesulfonic acid (BASA) (Chart I). In addition, the potential interaction of kringle 4 with benzamidine (Chart I), a ligand previously shown to have an affinity for kringle 5 (Vāradi & Patthy, 1981; Thewes et al., 1987, 1990), was investigated. By studying this set of analogues, our aim was to assess (a) the extent to which hydrophobic interactions contribute to the kringle 4 binding affinity with aromatic ligands and (b) the role of the ligand's ionic groups in the interaction with kringle 4.

Finally, we have also investigated the binding of L-arginine and its blocked derivatives (Chart II) to kringle 4. The major incentive for this study is the recent observation that kringle 4 exists as a dimer in the crystalline state. The dimer structure is apparently stabilized by the cofacial interaction of Arg^{32} and Arg^{71} from one kringle 4 molecule with Asp^{55} and Asp^{57} from the neighboring kringle 4 molecule (Mulichak & Tulinsky, 1990). Furthermore, a weak association of kringle 4 with L-arginine ($K_a \sim 0.08$ mM^{-1}) has been previously reported (Novokhatny et al., 1989). This interaction was not detected via affinity chromatography experiments (Winn et al., 1980).

The present studies extend the range of kringle 4 ligands previously investigated in our laboratories (De Marco et al., 1987; Ramesh et al., 1987; Petros et al., 1989) and are expected to improve our understanding of the role of plasminogen in the fibrinolytic cascade. Such knowledge ought to assist in assessing potential ligands as antifibrinolytic drugs (Markwardt, 1978) and in designing strategies to control plasmin(ogen) activity in vivo.

Experimental Procedures

Protein Purification and Sample Preparation. Human plasminogen was purified from aged, citrated plasma (Central Blood Bank of Pittsburgh, Pittsburgh, PA) according to the method of Deutsch and Mertz (1970). Kringle 4 was prepared via elastase digestion of human plasminogen and affinity chromatography on lysine-Sepharose, followed by cation exchange chromatography on CM-Sephadex and dialysis at pH 4.0, as previously described (Petros et al., 1989). CM-Sephadex, 1-aminohexane, benzylamine, 1-hexanoic acid, *p*-toluic acid, AMCHA, and 5-APA were obtained from Sigma (St. Louis, MO). 7-AHA was purchased from Pfaltz & Bauer (Waterbury, CT). BASA belonged to a batch previously described (Hochschwender et al., 1983). PAMBA was provided by Dr. R. Laursen (Boston University). NMR spectra of the ligands were recorded to check for the presence of impurities. No substantial amount of impurities (>0.1%) were detected in any of them. All commercial ligands were spectroscopic grade.

Prior to acquisition of NMR data, kringle 4 samples were dissolved in ^2H_2O, and labile hydrogen atoms were allowed to exchange with solvent deuterons for 3–4 h at 37 °C. The samples were then lyophilized exhaustively to remove residual $^1H^2HO$. Typically, 0.4 mL of 1 mM protein solutions adjusted to pH* 7.2 were used for ligand titrations at 24 °C. A 2 mM kringle 4 solution containing 1.6 mM AMCHA was used for two-dimensional (2D) experiments on the kringle 4/AMCHA complex.

NMR Spectroscopy. ^1H NMR spectra were acquired in the Fourier mode with quadrature detection using a Bruker WM-300 or AM-500 spectrometer operating at 300 and 500 MHz, respectively. The residual $^1H^2HO$ signal was suppressed by selective gated irradiation for 1.2 s between scans; 1000–3000 (300 MHz) or 48–96 (500 MHz) transients were collected at each titration point. Spectral widths were 5000 (300 MHz) or 6000 Hz (500 MHz). Resolution enhancement was achieved by Gaussian multiplication of the FID. Chemical shifts of specific resonances were determined with the peak-picking routine of the Bruker software package. Chemical shifts are referred to the sodium trimethylsilyl(2,2,3,3-^2H)-propionate line using *p*-dioxane as internal reference (De Marco, 1977). Two-dimensional chemical shift correlated (COSY) spectra (Nagayama et al., 1980; Wider et al., 1984) were acquired as described (Ramesh et al., 1987). 500-MHz 2D spectra of kringle 4 complexes with arginine derivatives and AMCHA were acquired in the phase-sensitive mode using time-proportional phase incrementation (TPPI) along ω_1 for the first pulse (Marion & Wüthrich, 1983). A total of 48–64 scans for each of 560–768 t_1 values were collected over 4096 data points in t_2. Zero-filling was used to extend the t_1 dimension. Unshifted sine bell window functions were applied in both dimensions for resolution enhancement.

A NOESY spectrum (Jeener et al., 1979; Bodenhausen et al., 1984) of the kringle 4/AMCHA complex was acquired at 500 MHz in the phase-sensitive mode (TPPI) with a 200-ms mixing time; 64 scans for each of 512 t_1 values were collected over 4096 data points in t_2. Data were processed on an Aspect X32 workstation using the UXNMR software package from Bruker. A squared sine bell window function shifted by 45° was applied in both dimensions for resolution enhancement.

Molecular Modeling. The kringle 4/AMCHA complex structure was generated using the molecular dynamics and energy minimization program XPLOR (Brünger, 1990). The model was built starting from the 1.8-Å X-ray crystallographic structure of ligand-free kringle 4 (Mulichak & Tulinsky, 1990). Observed kringle 4/AMCHA intermolecular and kringle 4 intramolecular NOEs were incorporated. We also included two artificial distance restraints in order to favor orienting the side-chain cationic groups of Lys^{36} and Arg^{71} toward the AMCHA carboxylate group. Missing hydrogen atoms from the original kringle 4 crystal structure were incorporated using the BUILD routine of CHARMM (Brooks et al., 1983). A model of the ligand AMCHA was generated starting from a lysine template and incorporating a cyclohexyl group using the topology file version TOPALLH6 of CHARMM.

The AMCHA molecule was manually fitted into the kringle 4 binding pocket with the DOCK facility of the molecular graphics program HYDRA (Hubbard, 1986). Then, the kringle 4/AMCHA system was subjected to a 1000-step restrained POWELL minimization using XPLOR. For the latter, use was made of (i) a square-well potential function to constrain NOE-derived upper and lower bound distances, (ii) uniform high values of the force constants for bond, angle, and improper terms, and (iii) the Lennard-Jones and the Coulombic electrostatic (with distance-dependent dielectric constants and with nonbonding cutoff = 8.5 Å) potentials to account for the nonbonding interactions.

Ligand docking was performed on a microVAX II computer interfaced with an Evans and Sutherland PS300 Graphics workstation. Otherwise, all computations were carried out on the Cray Y-MP computer of the Pittsburgh Supercomputing Center. Figures for the kringle 4/AMCHA complex were generated on a Silicon Graphics personal Iris 40/25 workstation with the program MOL17 (Sneddon, 1990).

Calculation of Association Constants. Ligand/kringle 4 association constants (K_a) were calculated assuming single-site binding and fast ligand exchange (Feeney et al., 1979; De Marco et al., 1987). On this basis, resonance shifts caused by ligand additions are described by

$$\Delta = \Delta_o \frac{[SK]}{[SK] + [K]} \quad (1)$$

where $\Delta = \delta - \delta_o$, $\Delta_o = \delta_b - \delta_f$, and δ, δ_f, and δ_b are, respectively, the observed (exchange-averaged), ligand-free, and ligand-saturated chemical shifts of a kringle resonance. [SK] and [K] are the concentrations of bound and free kringle, respectively. Data were fitted to the hyperbolic Langmuir adsorption equation

$$\Delta_p = \frac{K_a[S]}{1 + K_a[S]} \quad (2)$$

and/or to its linearized forms

$$S_o(\Delta_p^{-1} - 1) = K_a^{-1} + K_o(1 - \Delta_p) \quad (3)$$

$$\Delta_p^{-1} = 1 + 1/K_a(S_o - K_o\Delta_p) \quad (4)$$

where $\Delta_p = \Delta/\Delta_o$, $S_o = [SK] + [S]$, and $K_o = [SK] + [K]$.

For very weak binding ($K_a < 1$ mM^{-1}), it may be assumed that throughout the titration, the free-ligand concentration equals total ligand concentration (Sahai et al., 1974; Harris, 1986). In such cases, the NMR version of the Scatchard plot was used (Foster & Fyfe, 1969):

$$\Delta/S_o = -K_a\Delta + \Delta_o K_a \quad (5)$$

Plots of Δ/S_o versus Δ for each ligand-sensitive resonance are thus expected to yield straight lines whose slopes afford estimates of K_a. When more than one resonance was monitored, the reported K_a value represents the average of values derived from each titration profile.

Results

The low-field spectrum of kringle 4 (8.6–4.8 ppm) contains multiplets arising from the aromatic ring protons of the Trp, Phe, and Tyr residues. Singlet-like peaks arising from the His^3, His^{31}, and His^{33} side-chain imidazole ring H2 and H4 protons and from the Trp^{25}, Trp^{62}, and Trp^{72} side-chain indole ring H2 protons (De Marco et al., 1985, 1989; Motta et al., 1986; Ramesh et al., 1987) also appear in this region. The responses of these signals to ligand addition were monitored because of their sensitivity to ligand presence and ease of detection (De Marco et al., 1987).

Aromatic Ligands. Among the potential ligands BASA, PAMBA, benzylamine, *p*-toluic acid, and benzamidine (Chart I), only the first three bind measurably to kringle 4. Figure 1 illustrates the shifts of the singlet-like resonances described above upon saturation of kringle 4 with the ligand PAMBA. The shifts of the singlet-like peaks with increasing [ligand]/[kringle 4] ratios are plotted in Figure 2. Comparison to a similar plot for BASA (De Marco et al., 1987) and benzylamine (not shown) reveal that the Trp^{72} H2 singlet undergoes characteristically large shifts when in the presence of aromatic ligands. This effect may be attributed to an anisotropic ring current effect induced by the ligand on the Trp^{72} H2 resonance (De Marco et al., 1987). Indeed, ligand-to-kringle 4 ^{1}H NMR magnetization transfer (NOE) experiments on the BASA/kringle 4 complex have provided unambiguous evidence that the Trp^{72} side chain is in close contact with the ligand aromatic ring (De Marco et al., 1986b). This interaction is also revealed by the sensitivity of this proton to the negatively charged substituent on the BASA ring.

Figure 3A–D shows kringle 4 Trp indole CH–CH COSY connectivities, ligand-free and in the presence of saturating amounts of various aromatic ligands. As is apparent, the Trp^{72} H4, H5, H6, and H7 resonances are affected less than the corresponding H2 signal when in the presence of aromatic ligands. The various aromatic ligands seem to induce similar patterns of perturbation on Trp^{72}. In contrast, the ring multiplets of Trp^{62} are greatly perturbed by the presence of both BASA and PAMBA (Figure 3B,C). [Cross-peaks from Trp^{62} are broadened beyond detection in the presence of PAMBA at 37 °C but become visible at 55 °C (data not shown)]. Unlike Trp^{72}, the pattern of Trp^{62} perturbations varies widely depending on the effector structure. Finally, it should be noted that the Trp^{25} side chain appears to be the least sensitive to the nature of the aromatic ligand. Chemical shift changes caused by ligand complexation are listed in Table I.

The His^3 imidazole ring resonances have been found to provide a poor probe for monitoring ligand binding (De Marco et al., 1987; Petros et al., 1989), a result we confirm in these studies. Indeed, photo-CIDNP experiments show that His^3

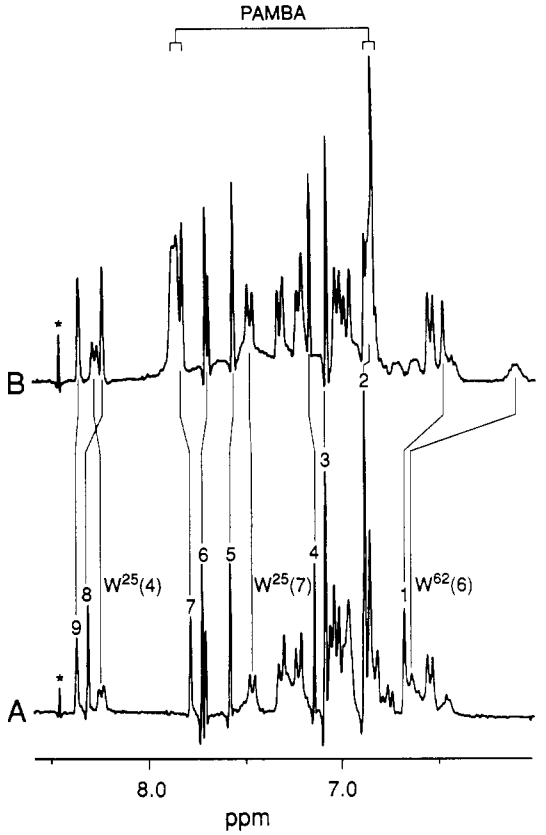

FIGURE 1: 300-MHz ^{1}H NMR aromatic spectrum of kringle 4: response to the ligand PAMBA. (A) Kringle 4 in the absence of ligand. Singlet-like peaks numbered 1–9 originate from Trp^{72} H2 (1), His^{33} H4 (2), His^{3} H4 (3), Trp^{25} H2 (4), His^{31} H2 (5), His^{3} H2 (6), Trp^{62} H2 (7), His^{33} H2 (8), and His^{31} H4 (9). (B) Kringle 4 in the presence of a 2-fold molar excess of PAMBA. Kinked vertical lines denote ligand-induced resonance shifts. The protein concentration is ~0.6 mM; the spectrum was recorded at 24 °C, pH 7.2. An asterisk indicates an impurity peak.

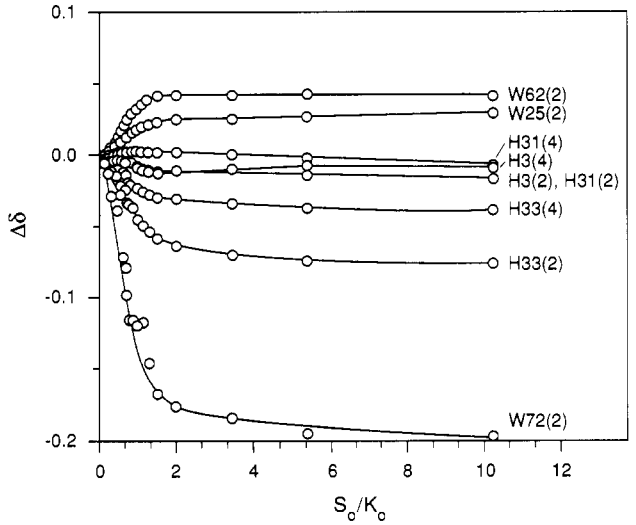

FIGURE 2: Ligand titration profiles of kringle 4 aromatic singlets with PAMBA. $\Delta\delta$ represents the difference between chemical shifts of kringle 4 singlet-like resonances recorded in the presence and absence of PAMBA. The ratio S_o/K_o is the molar ratio of total ligand to total kringle present in solution. Curves are labeled according to the one-letter amino acid code followed by the aromatic ring proton number (in parenthesis). A single curve (fifth from the top) delineates the movement of both His^3 H2 and His^{31} H2 resonances. Experimental conditions are as for Figure 1.

is a surface residue, not involved in interactions with ligands (De Marco et al., 1989). Similarly, the His^{31} H2 signal is relatively insensitive to the aromatic effector. In contrast, His^{33} H2 and H4 resonances shift to high field in response to PAMBA additions, the chemical shifts reaching saturation values in parallel with all the Trp H2 singlets (Figure 2). The magnitude of the ligand-saturated His^{33} chemical shifts remains virtually unchanged on going from PAMBA to benzylamine, i.e., upon removal of the ligand carboxylate group. These observations suggest that His^{31} and His^{33} are peripheral to the LBS and that they sense ligand complexation indirectly.

Table I: Selected Ligand-Induced Shifts on Aromatic Kringle 4 Multiplets

		$\Delta\delta^a$ (ppm × 10^3)				
residue	proton	BASA	PAMBA	AcArg	5-APA	7-AHA
His^3	H2	−6	−2	−2	−7	−3
	H4	nm[b]	14	9	14	−1
His^{31}	H2	−15	−14	−33	−33	−30
	H4	10	−12	−43	−8	−49
His^{33}	H2	−115	−78	10	−46	−50
	H4	−36	−29	22	−17	−42
Tyr^2	H2,6	−30	−28	−20	−10	−35
	H3,5	−2	4	−7	−17	11
Tyr^{41}	H2,6	−110	13	32	32	57
	H3,5	−18	7	−7	23	33
Tyr^{50}	H2,6	−9	−18	−7	−21	−14
	H3,5	3	5	22	5	8
Tyr^{74}	H2,6	22	−3	46	14	11
	H3,5	−5	−3	52	−58	−58
Phe^{64}	H2,6	14	nm[c]	−12	−62	148
	H3,5	186	141	54	4	−3
	H4	151	−225	81	21	−49
Trp^{25}	H4	29	6	32	32	72
	H5	46	−10	70	40	50
	H6	23	23	41	−52	23
	H7	12	−22	−19	−16	24
Trp^{62}	H4	183	nm[c]	−61	29	55
	H5	322	nm[c]	59	2	190
	H6	−459	−462	14	2	10
	H7	−496	nm[c]	−36	−166	67
Trp^{72}	H4	59	7	−50	5	95
	H5	−26	2	−53	−53	−103
	H6	61	−4	39	14	−28
	H7	−82	−93	151	111	111

[a] $\Delta\delta$ is the chemical shift of the kringle 4 resonance in the presence of saturating amounts of ligand relative to that in the absence of ligand. [b] Not measured; obscured by ligand signal. [c] Not measured; broadened beyond detection in the presence of ligand at 37 °C.

Figure 4 shows expansions of kringle 4 COSY aromatic spectra, with and without ligand. In general, the Tyr ring resonances are not much perturbed by ligand presence (Figure 4; Table I). BASA shifts Tyr^{41} the most, probably also an indirect effect on the aromatic side chain (Ramesh et al., 1987; Petros et al., 1989). As previously observed (Ramesh et al., 1987; Petros et al., 1989), Phe^{64} is most sensitive to the nature of the ligand. As for the Trp resonances, we find that the Phe^{64} H2,6 doublet broadens beyond detection in the presence of PAMBA at 37 °C. Such broadening is likely to stem from a ligand on/off exchange rate which matches the NMR chemical shift time scale, although a change in the Phe^{64} ring flipping rate cannot be excluded. Our data (Figure 4B–D) demonstrate that Phe^{64} is sensitive to the nature of the anionic (SO_3^- or COO^-) group attached to the aromatic ligand. This is consistent with the ability of the Phe^{64} side chain to sense the configuration about C$^\alpha$ on the enantiomers L- and D-lysine (Ramesh et al., 1987).

Aliphatic Analogues of 6-AHA. The ligands 1-aminohexane and 1-hexanoic acid were investigated to assess the contribution of the anionic and cationic ligand end groups to the interaction with kringle 4. In addition, the effect of ligand length was studied by resorting to 5-aminopentanoic acid (5-APA) and 7-aminoheptanoic acid (7-AHA), two analogues

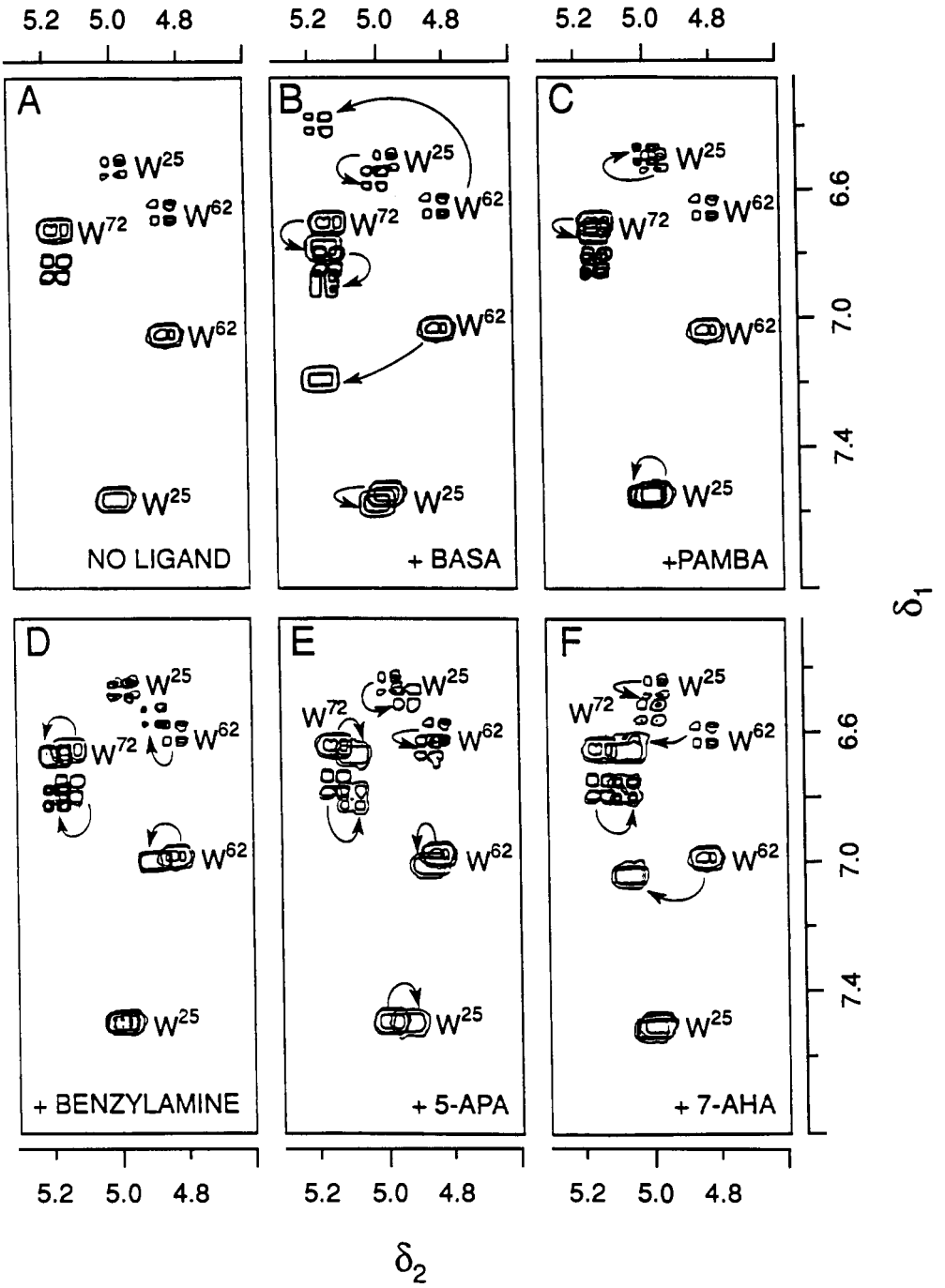

FIGURE 3: 300-MHz ^{1}H NMR COSY spectra of kringle 4: Trp side-chain response to ligand presence. (A) Kringle 4 in the absence of ligand; (B–F) kringle 4 in the presence of ligands BASA (B), PAMBA (C), benzylamine (D), 5-APA (E), and 7-AHA (F). To facilitate comparison, spectra of ligand-saturated kringle 4 are shown superimposed on its ligand-free spectrum. Arrows denote the direction of cross-peak shifts resulting from ligand addition. The kringle concentration is ~2 mM. Ligand/kringle 4 molar ratios range from 2:1 to 3:1; except for benzylamine, these are saturating amounts of ligand. Spectra were recorded at pH* 7.2, 37 °C.

of 6-AHA. Of these ligands, only 1-hexanoic acid did not exhibit measurable binding to kringle 4. In contrast, 5-APA was found to possess a relatively higher affinity ($K_a \sim 16$ mM^{-1}) for the kringle. Figure 5 illustrates the shifts of the singlet-like aromatic resonances of kringle 4 with increasing [5-APA]/[kringle 4] ratios (S_o/K_o).

The Trp^{72} H2 singlet is sensitive to changes in ligand length, shifting twice as much with 7-AHA and 5-APA as with 6-AHA [see De Marco et al. (1987) for the titration of kringle 4 with 6-AHA]. The Trp^{72} H2 also appears to be more sensitive to the carboxylate group in the aliphatic ligands than in the aromatic ones, shifting to low field in the presence of 1-aminohexane, rather than to high field, as with other investigated ligands (not shown). In contrast, the Trp^{62} H2 singlet is fairly insensitive to effector identity, shifting to low field by ~0.05 ppm with all aromatic and aliphatic ligands investigated. However, the Trp^{62} indole H5 triplet responds selectively to the presence of 7-AHA ($\Delta\delta \sim 0.19$ ppm) or 5-APA ($\Delta\delta \sim 0.002$ ppm). As with the aromatic ligands, Trp^{25} resonances are uniformly perturbed by the aliphatic analogues of 6-AHA.

While the response of the His^{33} H4 resonance is virtually independent of whether the effector is aromatic or aliphatic, the corresponding H2 proton is somewhat sensitive to the presence of a carboxylate group in aliphatic ligands. In the case of His^{31} H4 and H2, there are noticeable differences in

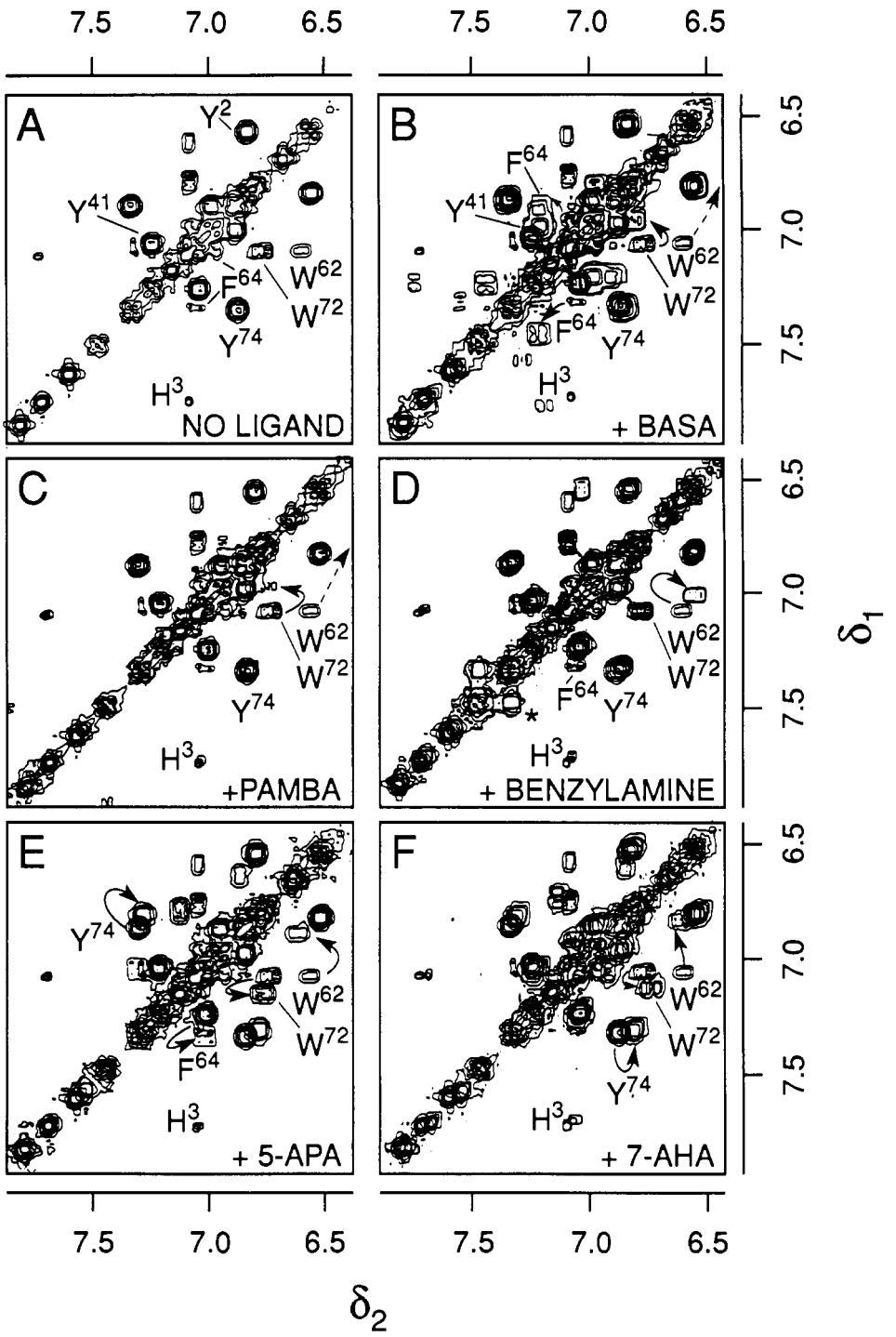

FIGURE 4: 300-MHz ^{1}H NMR COSY spectra of kringle 4: aromatic side-chain response to ligand presence. (A) Kringle 4 in the absence of ligand; (B–F) kringle 4 in the presence of ligands BASA (B), PAMBA (C), benzylamine (D), 5-APA (E), and 7-AHA (F). To facilitate comparison, spectra of ligand-saturated kringle 4 are shown superimposed on its ligand-free spectrum. An asterisk in spectrum D denotes a ligand cross-peak. Arrows denote cross-peak shifts resulting from ligand complexation. A dashed arrow trace indicates a Trp^{62} cross-peak which has shifted out of range (B). Experimental conditions are the same as for Figure 3.

$\Delta\delta$ on going from aromatic to aliphatic ligands (Figures 2, 5, and 6; Table I). Furthermore, the His^{31} H4 proton exhibits characteristic responses to 6-AHA (De Marco et al., 1987), 5-APA (Figure 5), and 7-AHA (not shown). There is also a slight increase in the His^{31} H4 $\Delta\delta$ value when 1-aminohexane is substituted for 6-AHA at the LBS.

The Tyr signals most perturbed by 5-APA and 7-AHA arise from Tyr^{74}. We note that this residue is more responsive to the aliphatic ligands than to the aromatic ones. Similar relative effects are observed for Phe^{64} H2,6, their signals shifting more markedly with 5-APA than with 7-AHA (Figure 4).

L-*Arginine and Its Analogues.* The interaction of kringle 4 with L-arginine, L-arginine methyl ester, N^{α}-acetyl-L-arginine, and N^{α}-acetyl-L-arginine methyl ester (Chart II) was investigated. Of these, only N^{α}-acetyl-L-arginine ($K_a \sim 0.32$ mM^{-1}) and N^{α}-acetyl-L-arginine methyl ester ($K_a \sim 0.08$ mM^{-1}) were found to bind measurably. Figure 6 shows the shifts of the kringle 4 singlet-like aromatic resonances with increasing levels of N^{α}-acetyl-L-arginine. Essentially the same changes in the kringle 4 aromatic spectrum are induced by N^{α}-acetyl-L-arginine and N^{α}-acetyl-L-arginine methyl ester. However, we note the following differences in the kringle 4

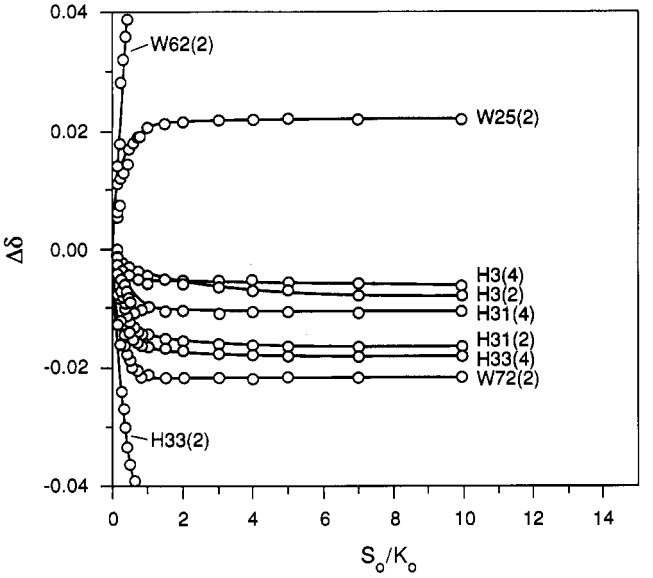

FIGURE 5: Titration of kringle 4 aromatic singlet-like peaks with 5-APA. Labels are the same as for Figure 2. Experimental conditions are as for Figure 1.

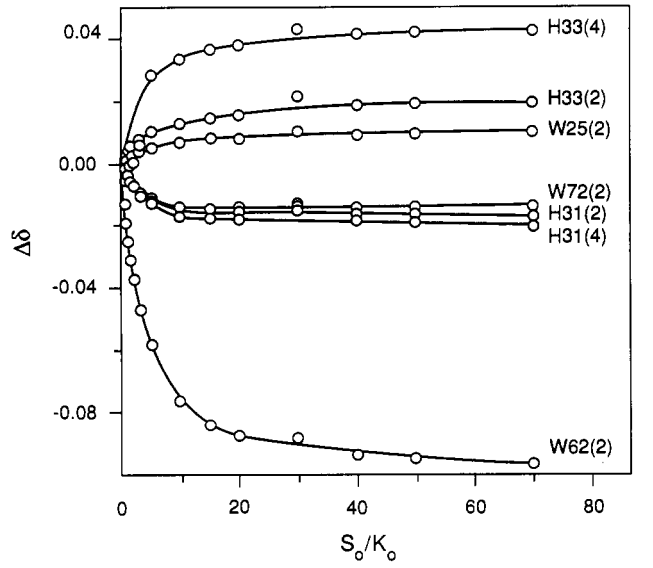

FIGURE 6: Response of kringle 4 aromatic singlet-like peaks to ligand: titration with N^{α}-acetyl-L-arginine. Labels are the same as for Figure 2. Experimental conditions are as for Figure 1.

response to ligand presence on going from the 6-AHA analogues to the arginyl compounds: (a) the Trp^{62} H2 singlet shifts to high field instead of to low field (Figures 5 and 6); (b) the Trp^{25} H2 singlet is relatively less perturbed when in the presence of arginyl ligands; and (c) His^{33} H2 is shifted to low field instead of to high field (Table I). In fact, of all the Trp residues, Trp^{62} seems to be the most characteristically affected by these ligands (Figure 7). Overall, the Tyr side chains are rather insensitive to the introduction of a guanidino group on the ligand (Figures 4 and 7). The shifts induced by N^{α}-acetyl-L-arginine on Phe^{64} H3,5 and H4 are larger than those caused by 5-APA and 7-AHA.

Kringle 4 Ligand-Binding Affinities. Ligand/kringle 4 association constants for 5-APA, 7-AHA, and PAMBA were calculated using eqs 2, 3, and 4 as described under Experimental Procedures; the linearized binding curves are shown in Figure 8A. For the weaker ligands 1-aminohexane, benzylamine, N^{α}-acetyl-L-arginine, and N^{α}-acetyl-L-arginine methyl ester, eq 5 was used. This treatment, applied to Trp^{25} H2 in the case of benzylamine and to Trp^{62} H2 in the case of N^{α}-acetyl-L-arginine, is illustrated in Figure 8B. Binding

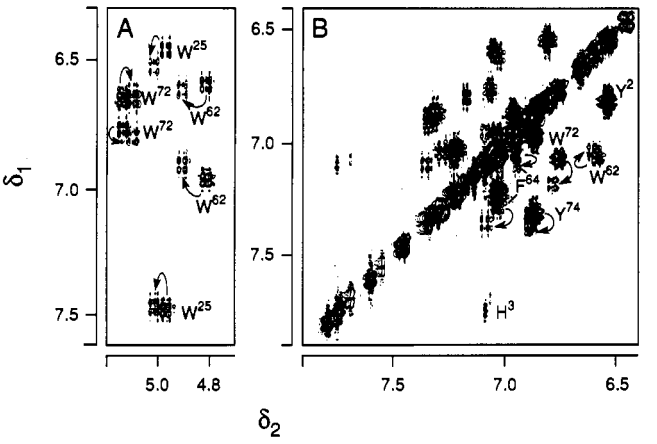

FIGURE 7: 500-MHz COSY spectrum of kringle 4: aromatic side-chain response to the presence of N^{α}-acetyl-L-arginine. (A) Trp indole ring cross-peaks; (B) Tyr and Phe ring cross-peaks. Spectra of ligand-bound kringle 4 have been superimposed on that of the ligand-free spectrum to facilitate comparison. Arrows show the direction of peak shifts induced by ligand complexation. The kringle 4 concentration is ~1 mM and the [ligand]/[kringle 4] ratio is ~20:1; the spectrum was recorded at 37 °C, pH* 7.2.

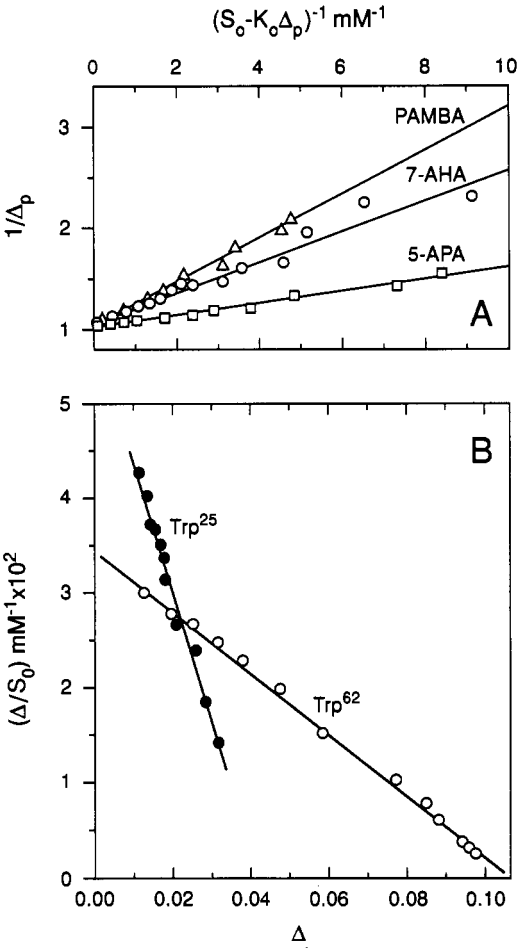

FIGURE 8: Linearized kringle 4 binding curves at 24 °C. (A) Ligands: PAMBA (Δ), 7-AHA (O), and 5-APA (□). Data are plotted according to eq 4. (B) Ligands: benzylamine and N^{α}-acetyl-L-arginine. Plots are according to eq 6. Data correspond to the Trp^{25} (●, benzylamine) and to the Trp^{62} (O, N^{α}-acetyl-L-arginine) H2 signals. In the case of benzylamine, similar plots were obtained for the His^{33} and Trp^{72} H2 signals. For N^{α}-acetyl-L-arginine, other Trp H2 resonances yielded similar plots. Association constant (K_a) values derived from these linear plots are listed in Table II.

Table II: Ligand/Kringle 4 Association Constants (K_a) Determined by NMR

ligand	K_a (mM^{-1})
7-AHA	6.62 ± 0.02
6-AHA	21 ± 1
5-APA	16 ± 1
1-aminohexane	0.07 ± 0.02
1-hexanoic acid	nb[a]
D-lysine[b]	1.2 ± 0.2
L-lysine[b]	24.4 ± 2.5
N^{α}-acetyl-L-lysine[c]	37 ± 1
L-lysine methyl ester[d]	1.5 ± 0.3
N^{α}-acetyl-L-lysine methyl ester[d]	0.2 ± 0.0
L-lysine hydroxamic acid[d]	2.0 ± 0.03
L-arginine	nb[a]
L-arginine methyl ester	nb[a]
N^{α}-acetyl-L-arginine	0.32 ± 0.02
N^{α}-acetyl-L-arginine methyl ester	0.08 ± 0.01
AMCHA[c]	159 ± 2
AMBOC[d]	48 ± 2
BASA[e]	74
PAMBA	4.8 ± 0.2
benzylamine	0.18 ± 0.03
p-toluic acid	nb[a]
benzamidine	nb[a]

[a] No specific binding (K_a < 0.05 mM^{-1}). [b] Ramesh et al. (1987). [c] De Marco et al. (1987). [d] Petros et al. (1989). [e] Hochschwender et al. (1983).

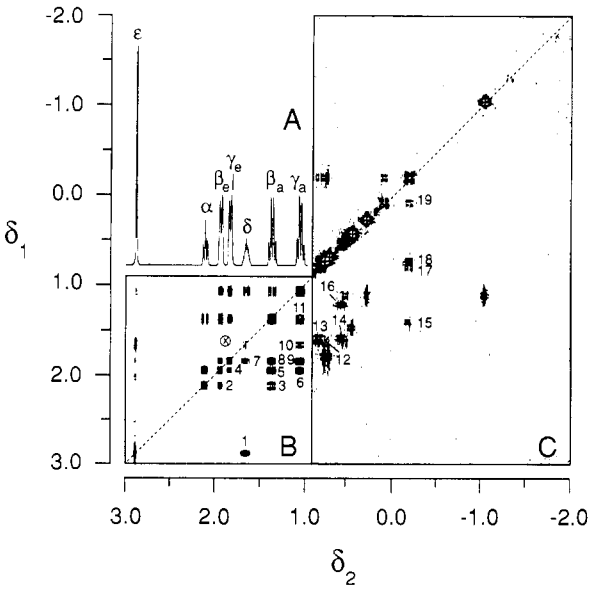

FIGURE 9: 500-MHz ^1H NMR spectra of AMCHA solution free and complexed to kringle 4. (A) 1D spectrum of AMCHA. The resonances are labeled according to Chart III. Assignments correspond to the chair conformation (Jackman & Sternhell, 1969). (B) Phase-sensitive COSY spectrum. Cross-peaks are numbered 1–11; assignments correspond to spectrum A (see Table IV). (C) COSY spectrum of the AMCHA/kringle 4 complex: high-field region. Numbered cross-peaks (12–19) originate from AMCHA protons in the kringle 4 bound state. Unlabeled peaks are from kringle 4 residues (Petros et al., 1988). The dashed line extending through panels B and C indicates the diagonal. All spectra were recorded at 37 °C, pH 7.2. In panels A and B the sample was ~30 mM in ^2H_2O; in (C) it was 2 mM in kringle 4 and 1.6 mM in AMCHA.

constants are listed in Table II.

Studies on the Kringle 4/AMCHA Complex. The antifibrinolytic drug, *trans*-(aminomethyl)cyclohexanecarboxylic acid (AMCHA) has a high affinity for kringle 4 (K_a ~ 159 mM^{-1}) (Markus et al., 1978; De Marco et al., 1987), exhibiting well-resolved signals in the kringle-bound state, quite distinct from those of the protein. Thus, AMCHA affords a most

Chart III

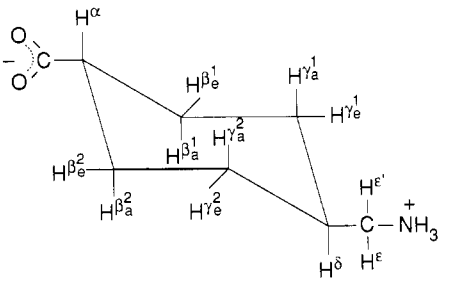

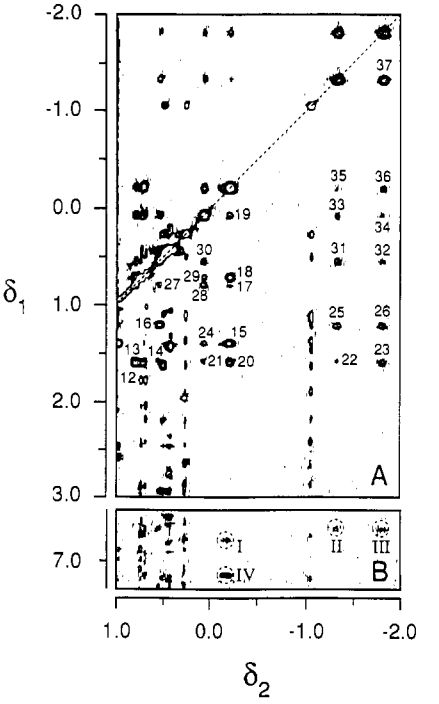

FIGURE 10: 500-MHz ^1H NMR NOESY spectrum of the AMCHA/kringle 4 complex. (A) High-field region: cross-peaks representing intramolecular AMCHA connectivities are numbered 12–37. Cross-peaks 12–19 are also observed in the COSY spectrum (Figure 9C). Unlabeled cross-peaks are intramolecular kringle 4 connectivities. (B) Intermolecular (kringle 4-AMCHA) connectivities. Cross-peaks encircled by a dashed line indicate NOESY connectivities between Trp^{72} H7 and $H\gamma_a^2$ (I), Trp^{62} H6 and $H\gamma_e^1$ (II), Trp^{62} H6 and $H\gamma_a^1$ (III), and Trp^{72} H6 and $H\gamma_a^2$ (IV). Experimental conditions are the same as for Figure 9. The NOESY experiment was acquired with a mixing time of 200 ms.

suitable probe to investigate ligand behavior when bound to kringle 4.

The structure of AMCHA and the labeling of its protons are defined in Chart III. The 1D and 2D COSY spectra of AMCHA (Figure 9A,B) show that, as expected from symmetry, the β_e, β_a, γ_e, and γ_a protons are pairwise magnetically equivalent. However, upon binding to kringle 4, the ligand spectrum shifts markedly to high fields, and these pairs of protons lose their magnetic equivalence (Figure 9B–C). Comparison of the COSY (Figure 9C) and NOESY (Figure 10) spectra of kringle-bound AMCHA and knowledge of its structure yield the chemical shift assignments listed in Table III.

The chemical shifts induced by kringle 4 on AMCHA (-3.073 ppm $\leq \Delta\delta \leq -0.325$ ppm) afford unambiguous evidence that the ligand ring intimately interacts with aromatic side chains at the binding site, in a stereospecific fashion. Furthermore, the NOESY connectivities between the AMCHA molecule and the Trp^{62} and Trp^{72} of kringle 4 (Figure 10B; peaks I–IV) indicate that the two indole groups contact

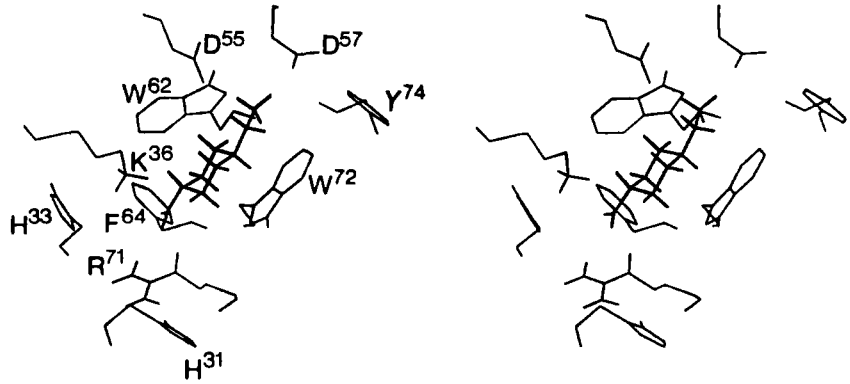

FIGURE 11: Kringle 4 lysine-binding site. The model incorporates ^{1}H NMR NOE restraints (Table IV) and is based on the plasminogen kringle 4 X-ray crystallographic structure (Mulichak & Tulinsky, 1991). The model features structural elements His[31], His[33], Lys[36], Asp[55], Asp[57], Trp[62], Phe[64], Arg[71], Trp[72], and Tyr[74]. AMCHA is shown in bold trace. Residues mentioned in the text are identified according to the one-letter amino acid code and their numbering in the primary sequence (Hochschwender et al., 1983).

Table III: AMCHA Resonances: Assignments and Kringle 4 Induced Shifts

proton[a]	cross-peaks COSY	cross-peaks NOESY	δ_{free} (ppm)	$\Delta\delta^b$ (ppm)
Hα	2-3, 13-14	13-14, 21-23	2.118	-0.508
Hβ_e^1	16	16, 25-26	1.945	-0.735
Hβ_a^1	14, 16	14, 16, 27, 30-32	1.364	-0.714
Hγ_e^1		22, 25, 31, 33, 35, 37	1.836	-3.169
Hγ_a^1		23, 26, 32, 34, 36-37	1.064	-2.874
Hβ_e^2	12	12, 20	1.945	-0.325
Hβ_a^2	12-13, 17	12-13, 17, 27-28	1.364	-0.564
Hγ_e^2	18	18, 29	1.836	-1.126
Hγ_a^2	17-19	17-20, 35-36	1.064	-1.264
Hδ	19	19, 21, 24, 28-30, 33-34	1.654	-1.564
Hϵ	15	15, 24	2.873	-1.463
Hϵ'	15	15	2.873	-3.073

[a] Superscripts distinguish sets of β and γ protons on the same side of the ring. This distinction can be made for kringle 4 bound AMCHA, but not for its free form. [b] Chemical shift of kringle 4 complexed minus protein-free AMCHA.

opposite sides of the ligand cyclohexane ring.

Discussion

Substitution of the sulfonate group in BASA by a carboxylate group in PAMBA reduces the K_a from 74 to 4.8 mM^{-1}, indicating a marked sensitivity of kringle 4 to the nature of the ligand anionic group. The stereochemistry of the sulfonate anion has been shown to play a crucial role in its recognition by various proteins (Luecke & Quiocho, 1985; Kanyo & Christianson, 1991). Thus, the kringle 4 preference for BASA may reflect a distinction between the different geometries of the carboxylate and sulfonate anions the former being planar and the latter pyramidal. It cannot be excluded that differences in solvation free energies between the two anions may also contribute to the observed effects.

The binding affinities of kringle 4 for 6-AHA ($K_a \sim 21$ mM^{-1}) and PAMBA ($K_a \sim 4.8$ mM^{-1}) indicate a substantial preference for the linear aliphatic chain ligand. This result is surprising considering previous reports that PAMBA possesses about 5 times the antifibrinolytic activity of 6-AHA (Okamoto et al., 1968; Markwardt, 1978). Thus, it is suggested that PAMBA interferes with fibrinolysis through interactions with regions of plasminogen other than just the kringle 4 module. Increasing the aliphatic ligand chain length by a methylene unit (~1 Å), as in going from 6-AHA to 7-AHA, decreases K_a from ~21 to ~6.6 mM^{-1}. Similarly, the ligand 5-APA, one methylene unit shorter than 6-AHA, exhibits a $K_a \sim 16$ mM^{-1}. These results, combined with those previously reported by Winn et al. (1980) and by Petros et al. (1989), underscore the existence of an optimal ligand fit at the binding site. Our results also corroborate the observation that there is no substantial difference between the binding strengths of 5-APA and 6-AHA. Similarly, the relative affinities of 5-APA, 6-AHA, and 7-AHA for kringle 4 shown here concur with those determined via calorimetry by Sehl and Castellino (1990), although the K_a values reported by these authors are nearly double in magnitude compared to those obtained by equilibrium dialysis and ^{1}H NMR experiments[2] (Lerch et al., 1980; De Marco et al., 1987).

The ligand structural requirements of each of the kringles studied thus far is effectively demonstrated by comparing plasminogen kringle 4 to t-PA kringle 2 and plasminogen kringle 5. In contrast to the human plasminogen kringle 4, t-PA kringle 2 exhibits a higher affinity for 7-AHA relative to 6-AHA (Cleary et al., 1989; Byeon, 1991). Furthermore, we find that benzamidine, a ligand for human plasminogen kringle 5 (Vâradi & Patthy, 1981; Thewes et al., 1987) exhibits no specific interaction with kringle 4. It has been shown previously that Asp[57] and Arg[71] are essential for the binding of kringle 4 (and probably other kringles as well) to ω-aminocarboxylic acids (Trexler et al., 1982). Indeed, any model of the kringle 4/AMCHA complex should incorporate the requirement that Asp[57] and Arg[71] contact the ligand amino and carboxylate groups, respectively. Figure 11 shows the X-ray crystallographic structure of the kringle 4 LBS, slightly modified by NMR-derived distance restraints (Table IV). The AMCHA ring is shown lying within a hydrophobic cleft formed by Trp[62], Phe[64], and Trp[72]. Also apparent from Figure 11 are the intermolecular ionic contacts between kringle 4 and the ligand. Asp[55] and Asp[57] are both close the the ϵ-amino group of AMCHA, while the Arg[71] and Lys[36] side chains anchor its carboxylate group. His[31], His[33], and Tyr[74] contribute to a secondary outer layer of the LBS. As discussed above (see Results), these residues show lesser sensitivity to structural differences among the ligands than Trp[62], Phe[64], and Trp[72] do, a manifestation of their greater distance from the ligand molecule.

We do not detect any binding of either L-arginine or L-arginine methyl ester to kringle 4. This is in contrast to the

[2] One possible factor which could account for higher K_a values frequently encountered in the literature is the presence of residual 6-AHA in the kringle 4 samples used for ligand titrations. NMR spectra of kringle 4, recorded at various stages in its purification, indicate that complete removal of the ligand 6-AHA is achieved only after cation exchange chromatography and exhaustive dialysis at pH 4.0.

Table IV: NOEs in the Kringle 4/AMCHA Complex

residue (*i*)	atom (*i*)	residue (*j*)	atom (*j*)	NOE[a]
Trp^{25}	H7	Leu^{46}	Hδ	++
Trp^{25}	H5	Leu^{46}	Hδ′	+
Trp^{25}	H5	Trp^{62}	H4	++++
Trp^{25}	H4	Trp^{62}	H4	++++
Trp^{25}	H4	Phe^{64}	H2,6	+
Trp^{25}	H5	Phe^{64}	H4	++
His^{31}	H4	Phe^{64}	H4	+
His^{33}	H2	Phe^{64}	H2,6	+
His^{33}	H2	Phe^{64}	H3,5	+
Trp^{62}	Hβ	Phe^{64}	H4	+++
Trp^{62}	Hβ′	Phe^{64}	H4	+++
Trp^{62}	H6	Phe^{64}	H4	++++
Trp^{62}	H2	Phe^{64}	H3,5	+
Trp^{62}	Hβ	Phe^{64}	H4	+++
Trp^{62}	Hβ′	Trp^{72}	H4	+++
Trp^{62}	H4	Trp^{72}	Hβ	++
Trp^{62}	H4	Trp^{72}	Hβ′	++
Trp^{62}	H2	Trp^{72}	H4	++
Trp^{62}	H2	Trp^{72}	H5	++
Trp^{72}	H5	Tyr^{74}	H2,6	++
Trp^{72}	H6	Tyr^{74}	H2,6	++
Trp^{72}	H5	Tyr^{74}	H3,5	+++
Lys^{36}	Nζ	AMCHA	COO^-	++[b]
Arg^{71}	Nζ	AMCHA	COO^-	++[b]
Trp^{72}	H7	AMCHA	$H\gamma_a^2$	++
Trp^{72}	H6	AMCHA	$H\gamma_a^2$	++
Trp^{62}	H6	AMCHA	$H\gamma_a^2$	++
Trp^{62}	H6	AMCHA	$H\gamma_e^1$	++

[a] Strong (++++), medium (+++), weak (++), and very weak (+) NOEs are assigned upper distance limits of 3.5, 4.5, 6.0, and 7.0 Å, respectively. The lower limit in all cases is assigned a value of 1.8 Å. [b] Artificial NOEs introduced to initially dock the ligand at the binding site. They were removed in a second refinement step (see Experimental Procedures).

fluorescence studies of Novokhatny and co-workers (1989), who report $K_a \sim 0.08$ mM^{-1} for the kringle 4-arginine interaction, a magnitude normally measurable by ^1H NMR. Our results on L-arginine concur, however, with the inability of this amino acid to elute kringle 4 attached to lysine-Sepharose (Winn et al., 1980). Since relative to L-lysine, the L-arginine dipole is ~0.2 Å longer, the lack of measurable interaction between kringle 4 and L-arginine methyl ester most likely can be attributed to an electrostatic repulsion between the Arg^{71} and/or Lys36 side chains and the α-amino group of the ligand (Figure 11). It is suggested that this unfavorable contact is not compensated for by the ionic interaction between the ligand guanidino group and Asp^{55} and/or Asp^{57}. In kringle 5, the replacement of Arg^{71} by Leu, a neutral amino acid (Trexler et al., 1982), would result in the absence of the electrostatic repulsion in question. This is supported by the detection of measurable binding ($K_a \sim 0.3$ mM^{-1}) to kringle 5 (Thewes et al., 1990). The affinity of N^{α}-acetyl-L-arginine ($K_a \sim 0.32$ mM^{-1}) and N^{α}-acetyl-L-arginine methyl ester ($K_a \sim 0.08$ mM^{-1}) for kringle 4 further supports this conclusion. Since N^{α}-acetyl-L-arginine and N^{α}-acetyl-L-arginine methyl ester mimic C-terminal and internal arginyl residues, respectively, our observations imply that arginyl residues in these positions may potentially function as kringle 4 ligands. In the case of fibrin, the sequences flanking the exposed arginyl residues may further modulate the interactions at the kringle 4 LBS.

The ligands benzylamine and 1-aminohexane definitely bind to kringle 4, although with low affinities ($K_a \sim 0.18$ mM^{-1} and ~0.07 mM^{-1}, respectively). This suggests that the cationic end of the ligand molecule suffices to drive the complexation, irrespective of the nature of the hydrocarbon moiety. However, by lacking the potential to interact electrostatically with the Arg^{71} guanidino group, the free energy of binding may be diminished because of the requirement to displace water bound to the polar environment. This factor would not affect binding of these ligands in the case of kringle 5.

We observe that neither of the anionic analogues, 1-hexanoic acid nor *p*-toluic acid, binds to kringle 4 ($K_a < 0.05$ mM^{-1}). This further supports the view that it is mainly the ligand cationic group which determines the interaction with the LBS through ionic pairing with the Asp^{55} and Asp^{57} side chains. Analogous results are obtained for blocked lysyl analogues (Petros et al., 1989) and for pentylamine and pentanoic acid with kringle 4 (Novokhatny et al., 1989). Consistent with this interpretation is the observation that kringle 5, which carries both Asp^{55} and Asp^{57} at the LBS (Trexler et al., 1982), binds a number of cationic ligands (Thewes et al., 1990).

The structure of the kringle 4/AMCHA complex reveals the cyclohexane ring of the ligand to be sandwiched between the indole rings of Trp^{62} and Trp^{72} (Figure 11). These aromatic rings form a hydrophobic cleft which serves as the foundation of the kringle 4 LBS. The distances between Trp^{62} H6 and the AMCHA $H\gamma_e^1$ and $H\gamma_a^1$ are ~4.6 Å and ~5.9 Å, respectively (weak NOEs, Table IV). A comparable distance (4.2 Å) separates the Trp^{72} H7 and the AMCHA $H\gamma_e^2$ protons. The position of the ligand's cyclohexane group between the two indole rings explains the dramatic high-field anisotropic ring current effect of the AMCHA Hβ ($-0.735 \leq \Delta\delta \leq -0.325$) and Hγ ($-3.169 \leq \Delta\delta \leq -1.126$) resonances (Table III). The Trp^{62} and Trp^{72} side chains which are in closest contact with AMCHA are, in turn, the most strongly perturbed by ligand presence. The Trp^{25} indole group, in contrast, ~9.5 Å removed from the ligand cyclohexane ring, exhibits a diminished sensitivity to the ligand structure.

The Phe^{64} side chain is oriented perpendicularly with respect to the plane of the AMCHA ring, with its H4 proton pointing toward the ligand Hα. The ~3.5-Å separation between these two protons is consistent with the sensitivity of Phe^{64} to stereoisomerism about the ligand C^{α} position (Ramesh et al., 1987). The model of the complex (Figure 11) shows close contacts between the AMCHA amino group and the carboxylate groups of Asp^{55} and Asp^{57} (average distance ~3.2 Å). Also evident from the model is the proximity of the ligand carboxylate group to the ε-amino group of Lys^{36} and the guanidino group of Arg^{71}, although the former appears closer to the anionic group (2.8 Å for Lys^{36} vs 4.7 Å for Arg^{71}). It is worth noting that the kringle binding sites becomes somewhat distorted by the presence of AMCHA: the Trp^{62} and Trp^{72} indole rings are slightly farther apart in the complex when compared to their relative positions in the crystal structure of ligand-free kringle 4 (Mulichak & Tulinsky, 1990). Such perturbation is not surprising, considering the bulk and rigidity of the cyclic ligand.

Of all the tyrosyl residues, Tyr^{74} is positioned the closest to AMCHA (~8.2 Å, average distance between rings, Figure 11) and is quite sensitive to the aliphatic ligands (Figure 4E,F). In the model of the kringle 4/AMCHA complex, we find that His^{33} is closer to the ligand than His^{31} is (Figure 11), consistent with (a) its more marked perturbation by ligand presence (Figure 2) and (b) its sensitivity to the ligand anionic group. However, the His^{31} H4 is quite responsive to ligand length. This may reflect a secondary effect stemming from its contact with Arg^{71} (Figure 11).

Conclusions

In conjunction with previous investigations (Winn et al., 1980; De Marco et al., 1987; Petros et al., 1989; Sehl & Castellino, 1990), our study confirms the stringency of the ligand chain length requirements for optimal interaction with

the kringle 4 LBS. As shown by the affinity of AMCHA for kringle 4 ($K_a \sim 159$ mM^{-1}) relative to those of 5-PA ($K_a \sim 16$ mM^{-1}), 6-AHA ($K_a \sim 21$ mM^{-1}), and 7-AHA ($K_a \sim 6.62$ mM^{-1}), the kringle exhibits a preference for ligands of ~6.8-Å dipole length. Furthermore, we have been able to better characterize the ligand specificity of plasminogen kringle 4 relative to those of t-PA kringle 2 and plasminogen kringle 5. Thus, the t-PA kringle 2 LBS favors the ligand 7-AHA ($K_a \sim 34$ mM^{-1}) over 6-AHA ($K_a \sim 10$ mM^{-1}) (Cleary et al., 1989) whereas the reverse trend is observed for plasminogen kringle 4. Similarly, while benzamidine binds to kringle 5 ($K_a \sim 3.41$ mM^{-1}) (Thewes et al., 1990), it does not bind to kringle 4, suggesting that hydrophobic interactions with the ligand aromatic ring do not suffice to drive the complexation in the case of the latter. However, this type of interaction appears to be relevant for kringle 5, which lacks Arg^{71} at the LBS (Thewes et al., 1990).

Comparisons of the binding affinity of kringle 4 toward the ligands 6-AHA, 1-aminohexane, and hexanoic acid demonstrate a drastic reduction in binding strength (21 to 0.07 mM^{-1}) upon removal of the ligand anionic end group. Thus, although the cationic variant 1-aminohexane is still able to interact with the LBS, the presence of an anionic group is required for effective binding. This conclusion is reinforced by our studies with PAMBA, benzylamine, and *p*-toluic acid. We have also shown that a free arginine exhibits practically no binding to kringle 4, although a weak affinity was detected to N^{α}-acetyl-L-arginine and N^{α}-acetyl-L-arginine methyl ester. This implies that, provided flanking sequences are favorable, kringle 4 is potentially capable of mediating interactions with an internal arginyl residue in the process of plasmin(ogen) interaction with fibrin(ogen) (Rejante et al., 1991).

Acknowledgments

We thank Prof. A. Tulinksy for the crystallographic coordinates of kringle 4.

References

Atkinson, R. A., & Williams, R. J. P. (1990) *J. Mol. Biol. 212*, 541–552.

Bodenhausen, G., Kogler, H., & Ernst, R. R. (1984) *J. Magn. Reson. 58*, 370–388.

Brockway, W. J., & Castellino, F. J. (1972) *Arch. Biochem. Biophys. 151*, 194–199.

Brünger, A. T. (1990) XPLOR *Version 2.1 User Manual*, Yale University Press, New Haven, CT.

Byeon, I.-J. L. (1991) Doctoral Dissertation, Carnegie Mellon University, Pittsburgh, PA.

Castellino, F. J., Ploplis, V. A., Powell, J. R., & Strickland, D. K. (1981) *J. Biol. Chem. 256*, 4778–4782.

Cleary, S., Mulkerrin, M. G., & Kelley, R. F. (1989) *Biochemistry 28*, 1884–1891.

De Marco, A. (1977) *J. Magn. Reson. 26*, 527–528.

De Marco, A., Hochschwender, S. M., Laursen, R., & Llinás, M. (1982) *J. Biol. Chem. 257*, 12716–12721.

De Marco, A., Pluck, N. D., Bányai, L., Trexler, M., Laursen, R. A., Patthy, L., Llinás, M., & Williams, R. J. P. (1985) *Biochemistry 24*, 748–753.

De Marco, A., Laursen, R. A., & Llinás, M. (1986a) *Arch. Biochem. Biophys. 244*, 727–741.

De Marco, A., Zetta, L., Petros, A. M., Llinás, M., Boelens, R., & Kaptein, R. (1986b) *Biochemistry 25*, 7918–7923.

De Marco, A., Petros, A. M., Laursen, R. A., & Llinás, M. (1987) *Eur. Biophys. J. 14*, 359–368.

De Marco, A., Petros, A. M., Llinás, M., Kaptein, R., & Boelens, R. (1989) *Biochim. Biophys. Acta 994*, 121–137.

Deutsch, D. G., & Mertz, E. T. (1970) *Science 170*, 1095–1096.

Feeney, J., Batchelor, J. G., Albrand, J. P., & Roberts, G. C. K. (1979) *J. Magn. Reson. 33*, 519–529.

Foster, R., & Fyfe, C. A. (1969) *Prog. Nucl. Magn. Reson. Spectrosc. 4*, 1–5.

Harris, R. (1986) *Nuclear Magnetic Resonance Spectroscopy*, John Wiley and Sons, Inc., New York.

Hochschwender, S. M., Laursen, R. A., De Marco, A., & Llinás, M. (1983) *Arch. Biochem. Biophys. 223*, 58–67.

Hortin, G. L., Trimpe, B., & Fok, K. F. (1989) *Thromb. Res. 54*, 621–632.

Hubbard, R. (1986) HYDRA: *Harvard York Drawing Program*, University of York, Heslington, York.

Jackman, L. M., & Sternhell, S., (1969) *Applications of Nuclear Magnetic Resonance in Organic Chemistry*, Pergamon Press, Braunschweig.

Jeener, J., Meier, B. H., Bachmann, P., & Ernst, R. R. (1979) *J. Chem. Phys. 71*, 4546–4553.

Kanyo, Z., & Christianson, D. (1991) *J. Biol. Chem. 266*, 4264–4268.

Lerch, P., Rickli, E., Lergier, W., & Gillessen, D. (1980) *Eur. J. Biochem. 107*, 7–13.

Llinás, M., Motta, A., De Marco, A., & Laursen, R. A. (1985) *Proc. Int. Symp. Biomol. Struct. Interactions, Suppl. J. Biosci. 8*, 121–139.

Luecke, H., & Quiocho, F. A. (1990) *Nature 347*, 402–406.

Marion, D., & Wüthrich, K. (1983) *Biochem. Biophys. Res. Commun. 113*, 967–974.

Markus, G., DePasquale, J. L., & Wissler, F. C. (1978) *J. Biol. Chem. 253*, 727–732.

Markwardt, F. (1978) *Fibrinolytics and Antifibrinolytics* (Markwardt, F., Ed.) pp 511–577, Springer-Verlag, Berlin.

Motta, A., Laursen, R. A., & Llinás, M. (1986) *Biochemistry 25*, 7924–7931.

Motta, A., Laursen, R., Llinás, M., Tulinsky, A., & Park, C. H. (1987) *Biochemistry 26*, 3827–3836.

Mulichak, A. M., & Tulinsky, A. (1990) *Blood Coagulation Fibrinolysis 1*, 673–679.

Nagayama, A., Kumar, A., Wüthrich, K., & Ernst, R. (1980) *J. Magn. Reson. 40*, 321–334.

Novokhatny, V. V., Matsuka, Y. V., & Kudinov, S. A. (1989) *Thromb. Res. 53*, 243–252.

Okamoto, S., Oshiba, S., Mihara, H., & Okamoto, U. (1968) *Ann. N.Y. Acad. Sci. A*, 414–429.

Petros, A., Gyenes, M., Patthy, L., & Llinás, M. (1988) *Eur. J. Biochem. 170*, 549–563.

Petros, A., Ramesh, V., & Llinás, M. (1989) *Biochemistry 28*, 1368–1376.

Ramesh, V., Petros, A. M., Llinás, M., Tulinsky, A., & Park, C. H. (1987) *J. Mol. Biol. 198*, 481–498.

Rejante, M., Elliott, B. W., & Llinás, M. (1991) *Fibrinolysis 5*, 87–92.

Rickli, E. E., & Otavsky, W. I. (1975) *Eur. J. Biochem. 59*, 441–447.

Sahai, R., Loper, G. L., Lin, S. H., & Eyring, H. (1974) *Proc. Natl. Acad. Sci. U.S.A. 71*, 1499–1503.

Sehl, L., & Castellino, F. J. (1990) *J. Biol. Chem. 265*, 5481–5486.

Sneddon, S. F. (1990) *MolX: A Series of General Purpose Molecular Graphics Programs (Version 17)*, Department of Chemistry, Carnegie Mellon University.

Sottrup-Jensen, L., Claeys, H., Zajdel, M., Petersen, T. E., & Magnusson, S. (1978) *Prog. Chem. Fibrinolysis Thrombolysis 3*, 191–209.

Suenson, E., & Thorsen, S. (1981) *Biochem. J. 197*, 619–628.
Sugiyama, N., Sasaki, T., Iwamoto, M., & Abiko, Y. (1988) *Biochim. Biophys. Acta 952*, 1–7.
Thewes, T., Ramesh, V., Simplaceanu, E., & Llinás, M. (1987) *Biochim. Biophys. Acta 912*, 254–269.
Thewes, T., Constantine, K., Byeon, I., & Llinás, M. (1990) *J. Biol. Chem. 265*, 3906–3915.
Thorsen, S. (1975) *Biochim. Biophys. Acta 393*, 55–65.
Trexler, M., Vâli, Z., & Patthy, L. (1982) *J. Biol. Chem. 257*, 7401–7406.
Tulinsky, A. (1991) in Proceedings of the XIII International Society of Thrombosis and Haemostasis Congress, Amsterdam, *Thrombosis Haemostasis 66*, 16–31.
Tulinsky, A., Park, C. H., Mao, B., & Llinás, M. (1988) *Proteins: Struct., Funct., Genet. 3*, 85–96.
Vâli, Z., & Patthy, L. (1982) *J. Biol. Chem. 257*, 2104–2110.
Vâradi, A., & Patthy, L. (1981) *Biochem. Biophys. Res. Commun. 103*, 97–102.
Wider, G., Macura, S., Kumar, A., Ernst, R., & Wüthrich, K. (1984) *J. Magn. Reson. 56*, 207–234.
Wiman, B., Boman, L., & Collen, D. (1978) *Eur. J. Biochem. 87*, 143–146.
Wiman, B., Lijnen, H. R., & Collen, D. (1979) *Biochim. Biophys. Acta 579*, 142–154.
Winn, E., Hu, S. P., Hochschwender, S., & Laursen, R. (1980) *Eur. J. Biochem. 104*, 579–586.

Investigation of the Functional Role of Tryptophan-22 in *Escherichia coli* Dihydrofolate Reductase by Site-Directed Mutagenesis[†,‡]

Mark S. Warren,[§] Katherine A. Brown,[§] Martin F. Farnum,[§] Elizabeth E. Howell,[∥] and Joseph Kraut*[,§]

Department of Chemistry, University of California, San Diego, La Jolla, California 92093, and Department of Biochemistry, Walters Life Science Building, University of Tennessee, Knoxville, Tennessee 37996

Received June 4, 1991; Revised Manuscript Received August 22, 1991

ABSTRACT: We have applied site-directed mutagenesis methods to change the conserved tryptophan-22 in the substrate binding site of *Escherichia coli* dihydrofolate reductase to phenylalanine (W22F) and histidine (W22H). The crystal structure of the W22F mutant in a binary complex with the inhibitor methotrexate has been refined at 1.9-Å resolution. The W22F difference Fourier map and least-squares refinement show that structural effects of the mutation are confined to the immediate vicinity of position 22 and include an unanticipated 0.4-Å movement of the methionine-20 side chain. A conserved bound water-403, suspected to play a role in the protonation of substrate DHF, has *not* been displaced by the mutation despite the loss of a hydrogen bond with tryptophan-22. Steady-state kinetics, stopped-flow kinetics, and primary isotope effects indicate that both mutations increase the rate of product tetrahydrofolate release, the rate-limiting step in the case of the wild-type enzyme, while slowing the rate of hydride transfer to the point where it now becomes at least partially rate determining. Steady-state kinetics show that below pH 6.8, k_{cat} is elevated by up to 5-fold in the W22F mutant as compared with the wild-type enzyme, although $k_{cat}/K_{m(dihydrofolate)}$ is lower throughout the observed pH range. For the W22H mutant, both k_{cat} and $k_{cat}/K_{m(dihydrofolate)}$ are substantially lower than the corresponding wild-type values. While both mutations weaken dihydrofolate binding, cofactor NADPH binding is not significantly altered. Fitting of the kinetic pH profiles to a general protonation scheme suggests that the proton affinity of dihydrofolate may be enhanced upon binding to the enzyme. We suggest that the function of tryptophan-22 may be to properly position the side chain of methionine-20 with respect to N5 of the substrate dihydrofolate.

Dihydrofolate reductase (DHFR,[1] EC 1.5.1.3) catalyzes the NADPH-dependent reduction of 7,8-dihydrofolate (DHF) to 5,6,7,8-tetrahydrofolate (THF). This activity is required to maintain intracellular pools of THF and its derivatives, which are essential cofactors in the transfer of one-carbon units in the biosynthesis of thymidylate, purine nucleotides, and some amino acids. Inhibition of DHFR activity by folate analogues and related compounds is important in the treatment of several diseases. Examples of these clinically useful compounds include the anticancer drug methotrexate (MTX), the antibacterial agent trimethoprim, and the antimalarial drug pyrimethamine.

[†] Based on the Ph.D. dissertation of M.S.W., supported by NIH Grants GM10928 to J.K. and GM35308 to E.E.H.

[‡] The coordinates for the recombinant wild-type *E. coli* dihydrofolate reductase and the W22F mutant have been submitted to the Brookhaven Protein Data Bank and have been assigned entry numbers 1DRC and 2DRC, respectively.

* Author to whom correspondence should be addressed.
[§] University of California.
[∥] University of Tennessee.

[1] Abbreviations: DHFR, dihydrofolate reductase; DHF, dihydrofolate; THF, tetrahydrofolate; MTX, methotrexate; NADPH, nicotinamide adenine dinucleotide phosphate (reduced form); wt, wild type; W22F, Trp-22 → Phe mutant dihydrofolate reductase; W22H, Trp-22 → His mutant dihydrofolate reductase; lc:W21L, Trp-21 → Leu mutant *Lactobacillus casei* dihydrofolate reductase; m:W24R, Trp-24 → Arg mutant mouse dihydrofolate reductase; h:W24F, Trp-24 → Phe mutant human dihydrofolate reductase; *E. coli*, *Escherichia coli*; *L. casei*, *Lactobacillus casei*.

$$R_{sym} = \sum_{hkl} \frac{\sum_i |I_i - \bar{I}|}{\sum_i I_i}$$

$$R\text{-factor} = \frac{\sum_{hkl} |F_o - F_c|}{\sum_{hkl} F_o}$$

0006-2960/91/0430-11092$02.50/0